

Article

Experimental Investigation of a Free-Form Honed Cylinder Liner for Heavy-Duty Engines

Frederik Stelljes *, Florian Pohlmann-Tasche and Friedrich Dinkelacker 

Institute of Technical Combustion, Leibniz University of Hannover, An der Universität 1, 30823 Garbsen, Germany; tasche@itv.uni-hannover.de (F.P.-T.); dinkelacker@itv.uni-hannover.de (F.D.)
* Correspondence: stelljes@itv.uni-hannover.de

Abstract: For future internal combustion engines, driven by regenerative fuels, efficiency is more important than ever. One approach to reduce the losses inside the piston cylinder unit (PCU) is to improve the alignment of the liner and the piston. Therefore, a cylinder liner with a free form was developed at the Institute of Technical Combustion (ITV) of the Leibniz University Hannover which compensates radial and linear deformations along the stroke. The layout is based on a FEM simulation. The liner was manufactured by the Institute of Production Engineering and Machine Tools (IFW) of Leibniz University of Hannover with a novel turn-milling process. The liner was investigated on the heavy-duty Floating-Liner engine of ITV with a displacement of 1991 ccm and a bore diameter of 130 mm. The experimental results show improvement in the friction losses over the whole engine map in the range of 9% and up to 17.3% compared to a serial liner. Sealing efficiency could be improved up to 28.8%, depending on the operational point. Overall, the investigation aims for lower fuel consumption which would result in fewer emissions.

Keywords: tribology; friction; piston group; cylinder liner; honing; floating liner; internal combustion engine; heavy duty



Citation: Stelljes, F.; Pohlmann-Tasche, F.; Dinkelacker, F. Experimental Investigation of a Free-Form Honed Cylinder Liner for Heavy-Duty Engines. *Lubricants* **2024**, *12*, 132. <https://doi.org/10.3390/lubricants12040132>

Received: 12 March 2024
Revised: 9 April 2024
Accepted: 11 April 2024
Published: 16 April 2024



Copyright: © 2024 by the authors. Licensee MDPI, Basel, Switzerland. This article is an open access article distributed under the terms and conditions of the Creative Commons Attribution (CC BY) license (<https://creativecommons.org/licenses/by/4.0/>).

1. Introduction

The piston cylinder unit is the central part of an internal combustion engine and has significant influence on the mechanical and thermodynamic losses as well as the pollutant emissions resulting from the oil [1]. The piston assembly consists of the piston, piston rings and the cylinder liner. The piston, which follows a sinusoidal forced motion from the crankshaft, carries the piston rings in their respective ring grooves. The piston rings are responsible for sealing the combustion chamber from the crankcase and are in tribological contact with the cylinder liner. Due to additional motion forms (hereinafter referred to as piston secondary motion), the piston is also in direct frictional contact with the cylinder liner. The components of the piston assembly form a tribological multibody system; each component forms a tribological system. Due to the different boundary conditions of each system, varying manifestations of friction forces result. In the following discussion, the individual components are reduced to a collaborative tribological system, allowing a holistic consideration of the piston assembly, whereby the resulting friction is a combination of the respective frictional states. The piston speed (v_{Piston}), cylinder pressure (p_{cyl}) and the corresponding temperature (T_{cyl}) are the essential variables depending on the crankshaft angle during the stroke. Figure 1 exemplifies the variation in the boundary conditions during one working cycle and illustrates the complexity of the tribological investigation of the piston group.

Due to inhomogeneities resulting from the overall engine construction and uneven heat sources and sinks, deformations of the cylinder liner occur. The varying temperature distribution results, on the one hand, from heat flows from combustion combined with the cycle-dependent cooling performance of the coolant mass flow and, on the other hand, from

mechanical loads arising from combustion pressure and assembly [2–4]. However, some of these effects can be partially compensated during the production of the cylinder liner using honing processes with a pretensioned liner. Figure 2 illustrates on the left a schematic deformation of a cylinder liner in the hot state. The conical-shaped deformation causes a narrowing of the lubrication gap between the cylinder liner and the piston skirt in the region of the Bottom Dead Center (BDC). An advance approach regards this deformation with an inverse conical shape in the cold state, shown on the right in Figure 2. The advanced manufacturing process required for this is already partly applied in mass production [5].

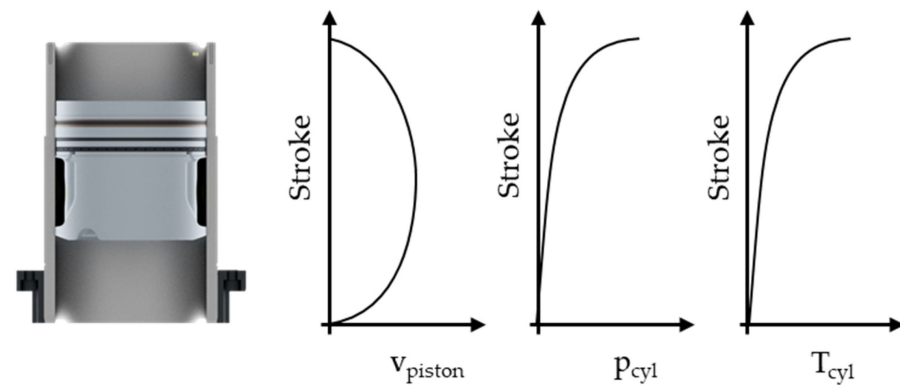


Figure 1. Boundary conditions depending on the stroke.

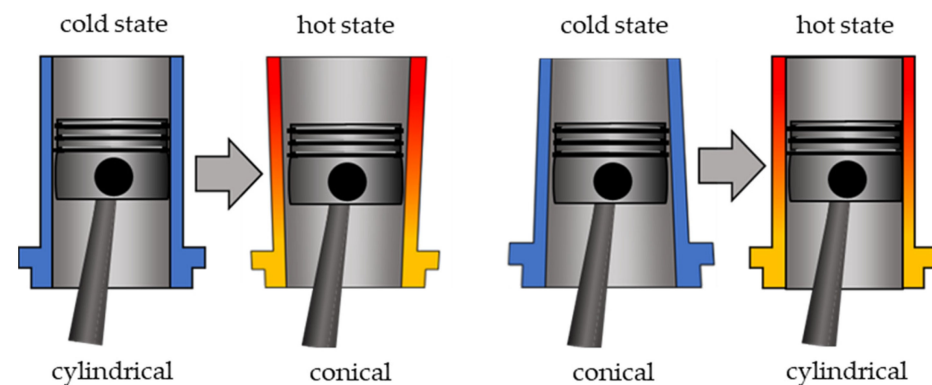


Figure 2. Principle of cylindrical contour honing, adapted from [5].

However, due to the varying wall thickness of the surrounding components and the resulting circumferentially changing heat transfer, different radial deformation forms are to be expected in the piston liner cross-section on each height (see Figure 3), which can be approximated by Fourier series [4]. During the operation of the internal combustion engine, uneven contact regions occur between the piston rings and the cylinder liner: this particularly affects the compression rings with tribological contact to the cylinder liner. In the presence of large clearances or lower-contact forces of the rings, leakages occur, negatively impacting the operation of the combustion chamber. Additionally, this can lead to oil entry into the combustion chamber (reverse blow-by) and it is one reason for higher emissions. Conversely, a tighter sealing results in a higher friction force [5–16].

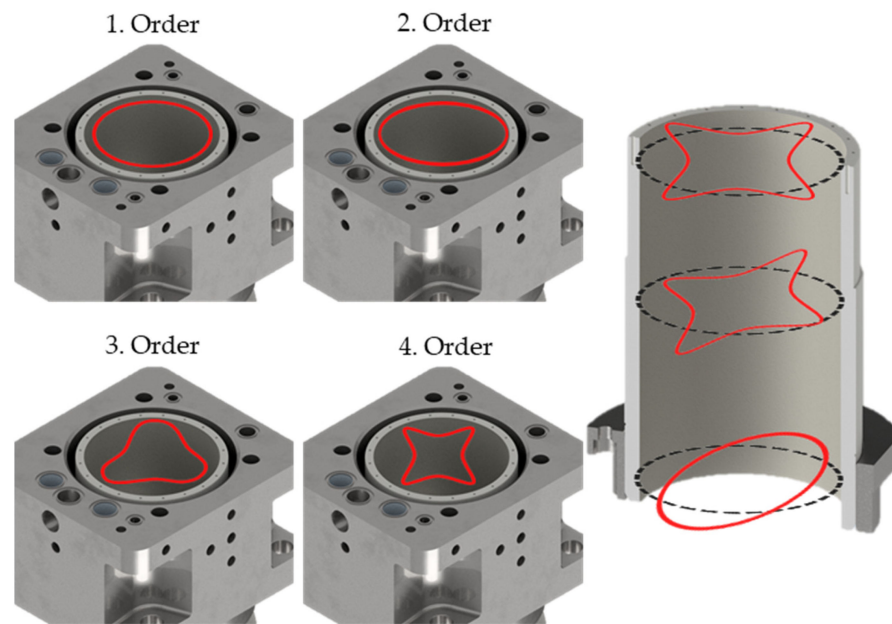


Figure 3. Deformation phenomena of cylinder liner (principle according to [15]).

As part of the “Powertrain 2025” project [17], cylinder liners are being developed to reduce energy consumption in both manufacturing and operational phases. Therefore, the geometry of the liner has been modified to minimize friction and leakage losses. Reduced friction force directly decreases the mechanical losses and is one part of internal combustion engine investigations for higher efficiencies and lower CO₂ emissions. The deformation of the cylinder liner from the Floating-Liner engine at the Institute for Technical Combustion (ITV) of Leibniz University Hannover is determined by simulations [17,18], based on finite element methods described in [19]. For this simulation, the thermal and mechanical load for one operation point (1300 rpm and 15.5 bar indicated mean effective pressure) is used. Based on this investigation, a free-form cylinder liner has been designed aiming to achieve a straight, cylindrical liner under warm-motored conditions. Subsequently, the liner was manufactured at the Institute of Production Engineering and Machine Tools (IFW) of Leibniz University Hannover with a novel milling process [17,20]. The aim of the study is to compare experimentally the friction forces for a reference liner, produced with a cylindrical form, and a liner produced with such a novel free-form honed liner design, which in the hot operation state is approximately cylindrical; also, the blow-by losses are determined [21–24]. In the following, at first the experimental setup is described with the test bench of the Floating-Liner single-cylinder engine. Then, more details of the two investigated liners and the investigated map of operation points are described, including an investigation of the experimentally determined deformation of the cylinder liner using strain gauges. Measurements of the two liners are described in a step-wise procedure: friction measurements with a disassembled cylinder head and motored engine for a first tribological characterization, and then friction measurements with an assembled cylinder head to investigate the influence of the combustion chamber pressure for motored and fired operations. In the Section 4, these data are analyzed, allowing a detailed analysis of the geometry influence on the friction contribution in the different process steps of the moving piston. Here, and in the Section 5, it will be discussed whether the following research questions can be answered: if a free-form cylinder liner design can reduce the friction from the piston group also in a broad range of operation conditions and if also the blow-by losses can be influenced.

2. Experimental Setup

2.1. Floating-Liner Testbench

In the laboratory at Leibniz University Hannover, a Floating-Liner single-cylinder test rig has been built up in recent years for detailed friction force measurements based on a commercial vehicle engine with a 130 mm bore with basic parameters given in Table 1 [25–28]. The Floating-Liner method is a direct measurement method for determining the frictional force between the piston assembly and cylinder liner. This method is fundamentally based on a liner that can move in the direction of the stroke. The liner is mounted in the stroke direction by using force sensors, allowing the crank-angle resolved measurement of the piston friction force (cf. [29–32]). The mechanical construction of a Floating-Liner requires significant design efforts in sealing the combustion chamber and in implementing measurement technology to eliminate disturbances during the measurement process. A hydrostatic bearing serves for the radial support and axial guidance of the liner in the liner housing, absorbing the occurring radial forces. The bearing is pressurized with externally conditioned hydraulic oil, supplying the hydraulic pockets. The supplied oil is guided back to the conditioning through a circulating drainage groove in the bearing. To seal the combustion chamber without axial force from the cylinder head mounting tension, the Floating-Liner at ITV is equipped with a gas-balancing system [15,16]. This system allows the effective combustion chamber pressure in the sealing area to be compensated, preventing force impact in the stroke direction and, thus, avoiding an influence on the measurement results. To implement this system, an equivalent compensating area is provided for the area in the combustion chamber sealing region between the roof ring and roof plate (see Figure 4). After every assembly, the cylinder unit is calibrated first for statical conditions and then for dynamical cases under comparable boundary conditions to the motored engine to compensate the effect of the sealing arrangement.

Table 1. Parameters of the single-cylinder research engine with Floating-Liner equipment.

Parameter	Unit	Value
Bore	mm	130
Stroke	mm	150
Displacement	ccm	1991
Max. speed	rpm	1600
Nominal power	kW	35
Max. peak cylinder pressure	bar	160
Fuel	-	Diesel

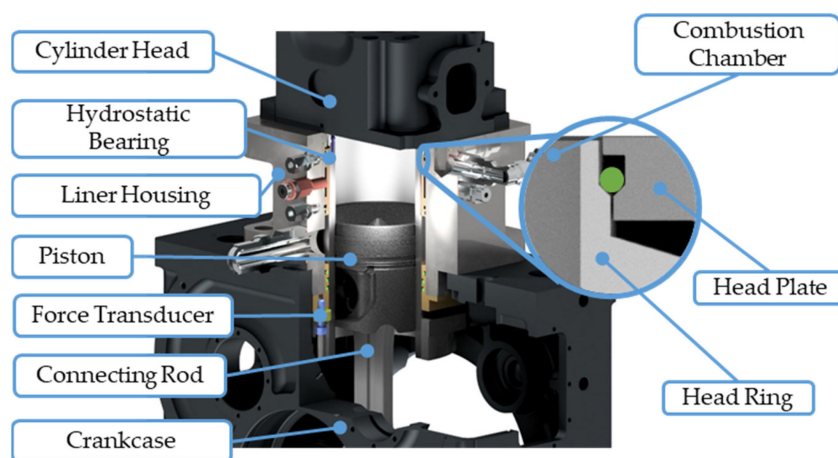


Figure 4. Floating-Liner, developed by [25,26].

2.2. Design Development of a Free Form Honed Liner

The basis of the new liner design is the simulation of the cylinder deformation under motored conditions at 1300 rpm and 15.5 bar IMEP (indicated mean effective pressure). Measurements of operating temperatures and pressures were conducted to establish boundary conditions. Additionally, the deformation of the cylinder liner is measured for this operation point with strain gauges at the height indicated by the yellow curve in Figure 5. The positions of the upper- and lower-edges of the piston are represented by the sinusoidal curve (purple and blue) and the cylinder pressure is plotted in red. The temperature of the cylinder liner on each height is assumed to be constant due to the high thermal mass.

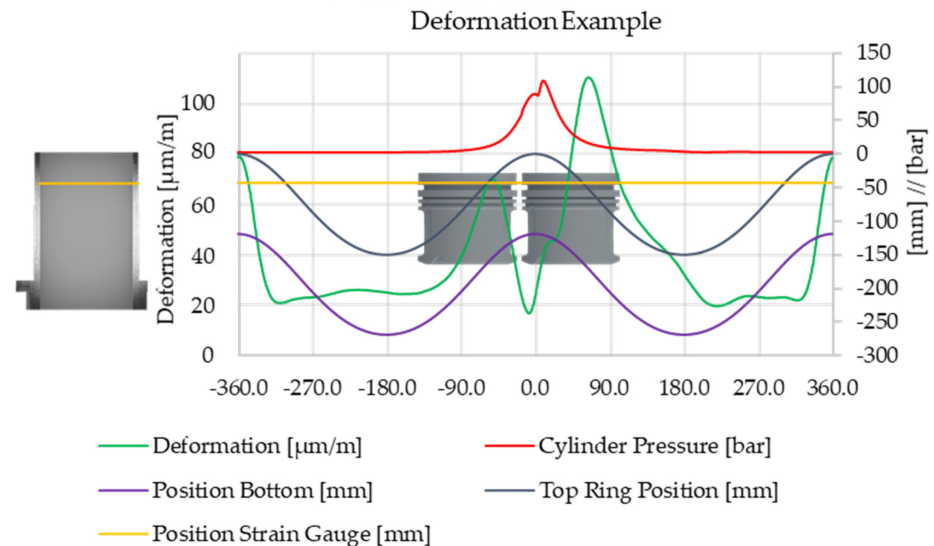


Figure 5. The deformation of the cylinder liner is determined using strain gauges. Example for 1000 rpm and 7.7 bar IMEP.

The deformation varies as a function of the piston position (green line). Essentially, it depends on three effects. Firstly, a static deformation results from the thermal influences and the assembly itself, forming a baseline at about $20 \mu\text{m}/\text{m}$. Secondly, the mechanical contact of the piston assembly increases the deformation, depending on the position of the piston. The third effect occurs from increasing pressure near combustion at the top dead center, which results in a higher deformation. Fundamentally, when the top ring passes the strain gauge the deformation is highly reduced by the sealing effects of the ring package. The varying amplitudes of the strain gauge signal result partly from the acting combustion chamber pressures but also from piston secondary movements.

Based on the knowledge of the deformation of the reference liner, the free-form liner is designed inversely that way to be straight and cylindrical at the hot operational state (Figure 6). The free-form liner has a maximum cylindrical deviation of 0.025 mm radial and a lateral deviation of 0.12 mm radial. To produce the developed form, a method was developed at the Institute of Manufacturing Technology and Machine Tools, enabling the creation of a machined free form during a machining step with an innovative machining tool [10]. The reference cylinder liner was manufactured close to series production. Despite the different shapes, the cylinder liners have similar surface roughness parameters.

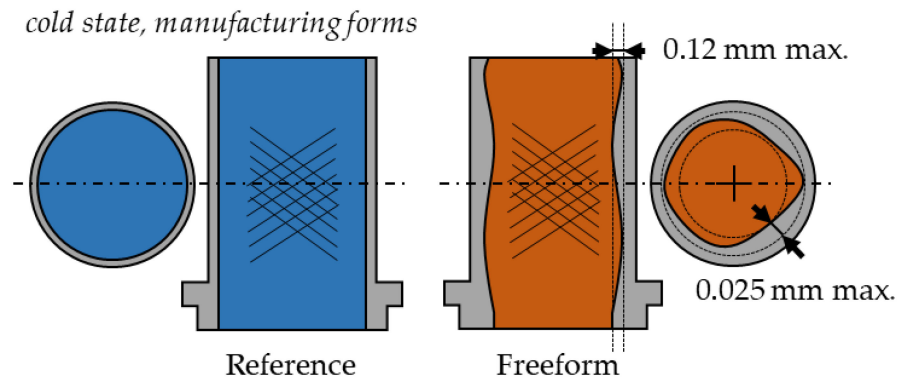


Figure 6. Investigated cylinder liner variations (strongly exaggerated presentation).

2.3. Boundary Conditions

The experimental study with the Floating-Liner engine covers different operational points. First, a study is performed without compression (cylinder head disassembled) for rotational speeds of 300/600/1000/1300/1600 rpm. The main experiments are performed with compression in a motored operation mode (presented by the negative IMEP, due to wall heat losses) and with different loads up to 15.5 bar IMEP for rotational speeds between 600 and 1600 rpm, as is shown in Figure 7.

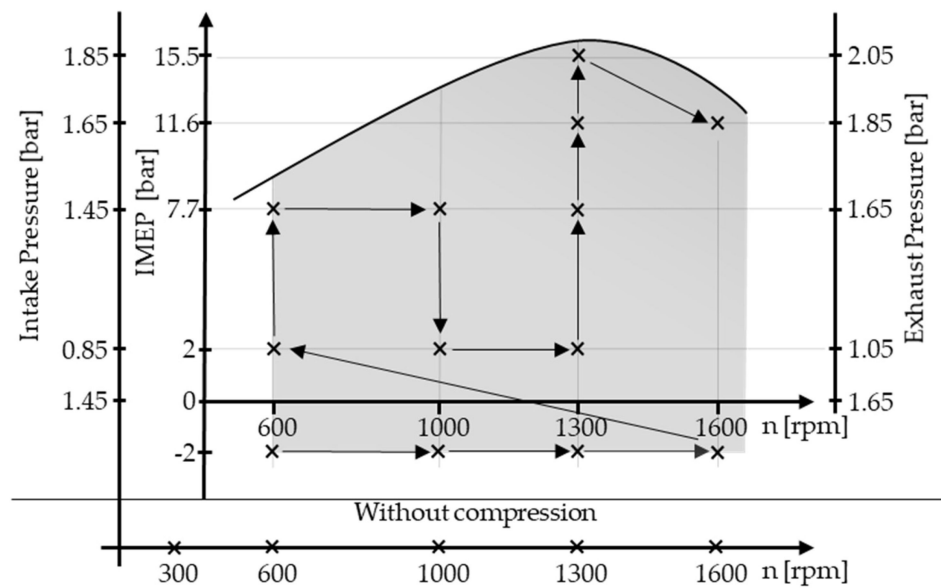


Figure 7. Loadpoints Floating-Liner experiments.

All medium flows supplying the Floating-Liner are externally conditioned. For precise friction results, it is important to control the pressures and temperatures exactly (with accuracies in the range of 0.1 °C and 0.05 bar). The values of the different parameters are given in Table 2.

Additionally, the same piston ring set, the same piston and the same oil are used for the investigations. This ensures that any disturbing influence on the tribological system from a variation in the components is prevented.

Table 2. Boundary conditions.

Parameter	Unit of Measurement
Intake temperature	50 °C
Coolant temperature	80 °C
Oil temperature	80 °C
Coolant flowrate	1200 L/h
Oil pressure piston cooling	4 bar
Oil pressure crank shaft	4 bar
Engine oil	15W40

3. Measurement Results

In the following, the friction force profiles of the cylinder liner variations are initially examined for measurements without pressure in the combustion chamber, followed by the corresponding profiles with the influence of cylinder pressure. For a detailed presentation of crank-angle resolved measured friction forces, only the operating points at $n = 600$ rpm are discussed here, as here a minimal influence from piston secondary movements and other disturbances is given. The profiles are derived from the averaged friction forces over 200 working cycles. Figure 8 depicts the friction force profile of the cylinder liner during a drag operation without compression, recorded by the two force sensors (the sum of the signals is shown).

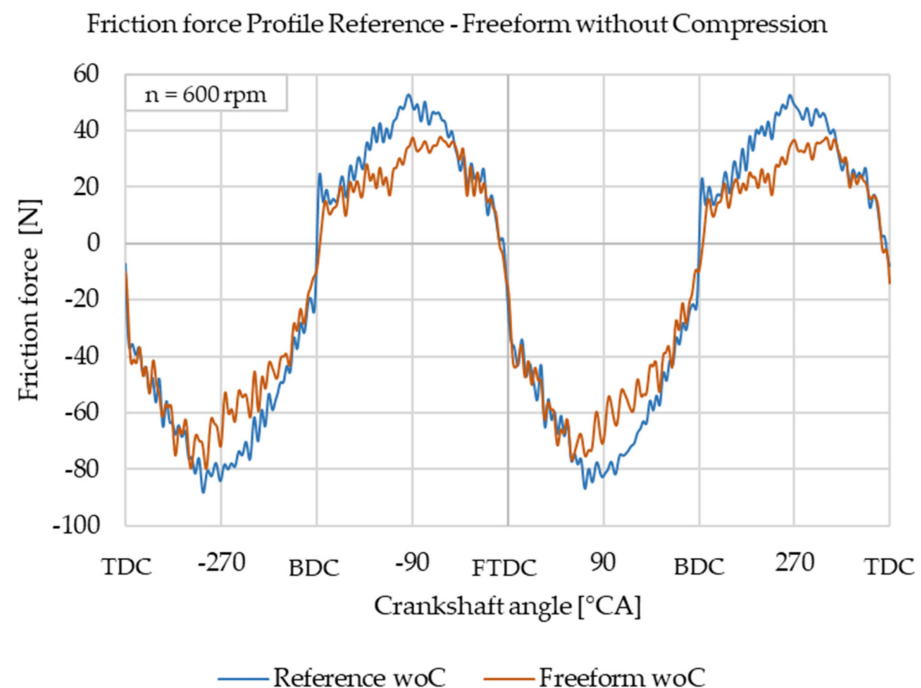


Figure 8. Crank-angle resolved friction force profile at 600 rpm without compression, measured with the Floating-Liner setup of ITV Hannover.

The measured friction force is plotted on the ordinate of the diagram, while the crankshaft angle is represented on the abscissa. The friction force is either positive when the piston movement is upwards directed or negative for the downwards movement. The friction value depends on the tribological process with fast jumps near the reversal points of the piston movement (dead center) and the piston movement speed in the hydrodynamic friction range with curved parts between the reversal points. Some oscillations are overlapping the force signal coming from vibration of the Floating-Liner system or the piston rings. The friction force of the reference liner is nearly symmetrically curved, while the free-form honed liner shows mostly lower friction, especially in the lower part of the liner, where the shape in this cold state is wider (see Figure 6). The reference liner

exhibits a pronounced friction force peak at the BDC (Bottom Dead Center). Analysis of other operating points without compression reveals that the free-form honed cylinder liner causes lower friction force across the entire speed range. Figure 9 shows the friction force profile with the cylinder head mounted, where at the FTDC (Fired Top Dead Center) the cylinder pressure rises to about 80 bar. Note that this is still an example without combustion (IMEP = −2 bar), so that the temperature of the liner is still rather low. Near the FTDC, the measured friction forces are significantly enhanced, reaching values of up to 400 N, compared to the much-lower forces for the cases without compression. This is expected from the mechanical influence of the cylinder pressure.

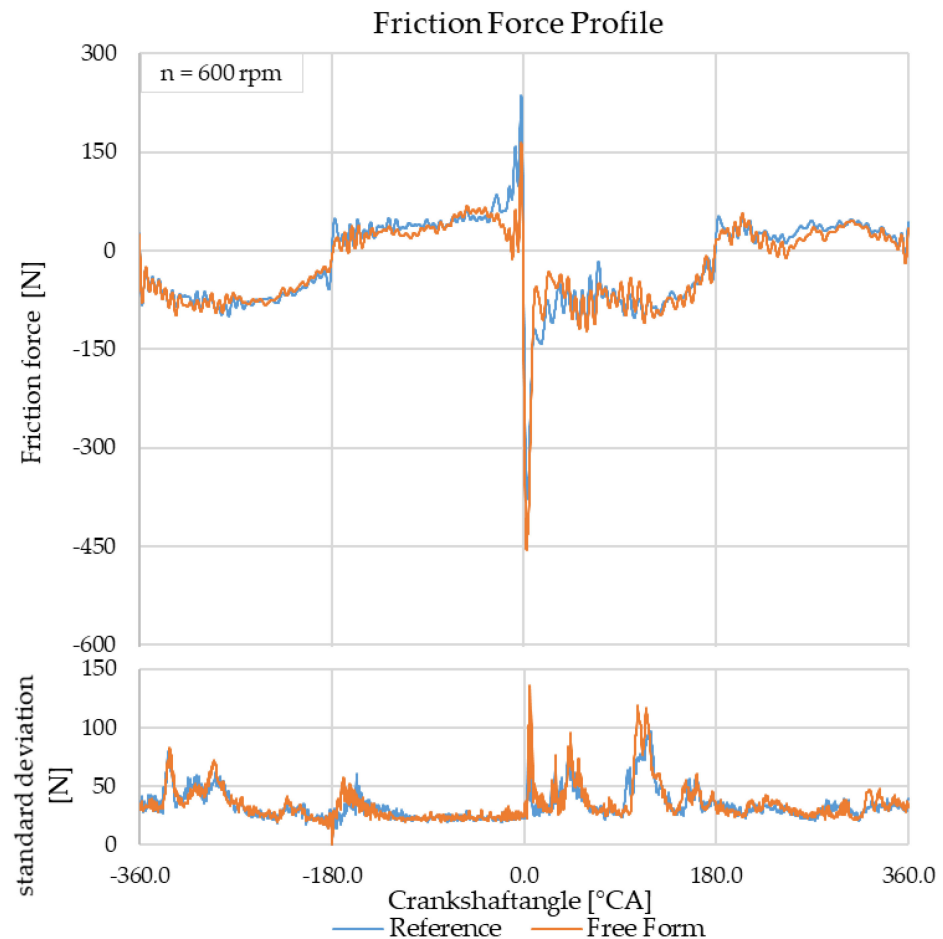


Figure 9. Crank-angle resolved friction force profile at 600 rpm with compression without combustion.

The curved profile between the reversal points is also observed in the measurements with compression pressure. The lower friction force level in the hydrodynamic area of the free-form honed liner is not clearly pronounced under the influence of cylinder pressure. Contrary to the operation without cylinder pressure, the friction force at the FTDC is at a higher level for the reference liner. The free-form honed liner exhibits a decreasing behavior in the range of -30°CA to 30°CA . The friction work of the piston group is determined by an integration of the measured friction force (F_p) and the speed of the piston (v_p) over the crank-angle φ resolved operation cycle (OC). The friction mean effective pressure of the piston (FMEP_p) results from the engine-displacement-related friction work.

$$FMEP_p = \frac{1}{V_d} \int_{OC} F_p(\varphi) \cdot v_P(\varphi) d\varphi = \frac{1}{V_d} \int_{OC} F_p(\varphi) \cdot r \left\{ \sin \varphi + \frac{(\lambda \cdot \sin \varphi \cdot \cos \varphi)}{\sqrt{1 - (\lambda \cdot \sin \varphi)^2}} \right\} d\varphi$$

Here, $\lambda = r/l$ is the ratio of the crank radius to the length of the rod, and V_d is the displacement volume of the cylinder. The piston velocity is calculated according to text books, e.g., [1,33,34].

Near the fired top dead center (FTDC), the friction force reaches its maximum; therefore, the value ΔF_{FTDC} is also evaluated. The friction mean effective pressure of the piston ($FMEP_p$) is a part of the total engine friction, commonly described by the mean effective pressure (FMEP) of the whole engine. The values $FMEP_p$ and the effective engine power P_e serve as references for the friction force measurements. Additionally, blow-by flow and the maximum cylinder pressure (p_{max}) are considered to assess the sealing of the combustion chamber against the crankcase.

The following measurements are presented in the engine map, where the engine speed is plotted on the abscissa and the indicated mean effective pressure (IMEP) is shown on the ordinate. This representation allows the investigation of load and speed dependencies of the measurement quantities. Figure 10 shows the measurement results of the cylinder liner with free-form honing. The total engine friction (friction mean effective pressure, FMEP) is determined from the difference between the measured break mean effective pressure, BMEP, and the measured indicated mean effective pressure, IMEP. It increases with higher engine speed for lower and medium load. For higher load and speeds of 1000 rpm and 1300 rpm, a significant reduction in total engine friction is observed with increasing IMEP. The $FMEP_p$, however, being determined from the measured forces of the Floating-Liner, exhibits a clear speed-dependent behavior, while only minor variations are found for varied load. The blow-by measurement is suitable only for higher speeds due to the measurement method. As a result, only a comparison of operating points around 1300 rpm and 1600 rpm is possible. For better characterizations of the blow-by, the measured values are normalized to the intake mass flow. The blow-by increases with rising IMEP but shows only a weak dependency on engine speed. The cylinder peak pressure shows a behavior equivalent to effective power (P_e). The friction force height at the fired top dead center ΔF_{FTDC} decreases with increasing speed during motored operation. For fired operating points, a reversed behavior is noticeable, with an alternating pattern observed at an IMEP of 7.7 bar. In terms of increasing IMEP, the ΔF_{FTDC} value rises. The largest amplitude is observed at a speed of 1300 rpm and an IMEP of 15.5 bar.

The measurement results for the reference liner are shown in Figure 11. The friction contribution FMEP reaches its minimum at the lowest load points, increasing at higher speeds and IMEP. The drag operation points show increased friction for the piston group compared to points with identical speeds but at higher indicated mean pressures. The friction of the piston group also increases with higher speeds. The effective power, maximum cylinder pressure and force jump at the FTDC exhibit similar trends to the cylinder liner with free-form honing. The blow-by reaches its minimum at an engine speed of $n = 1600$ rpm. At an engine speed of $n = 1300$ rpm, a swelling behavior of blow-by is noticeable, while a reduction in leakage in the middle load range is distinguishable.

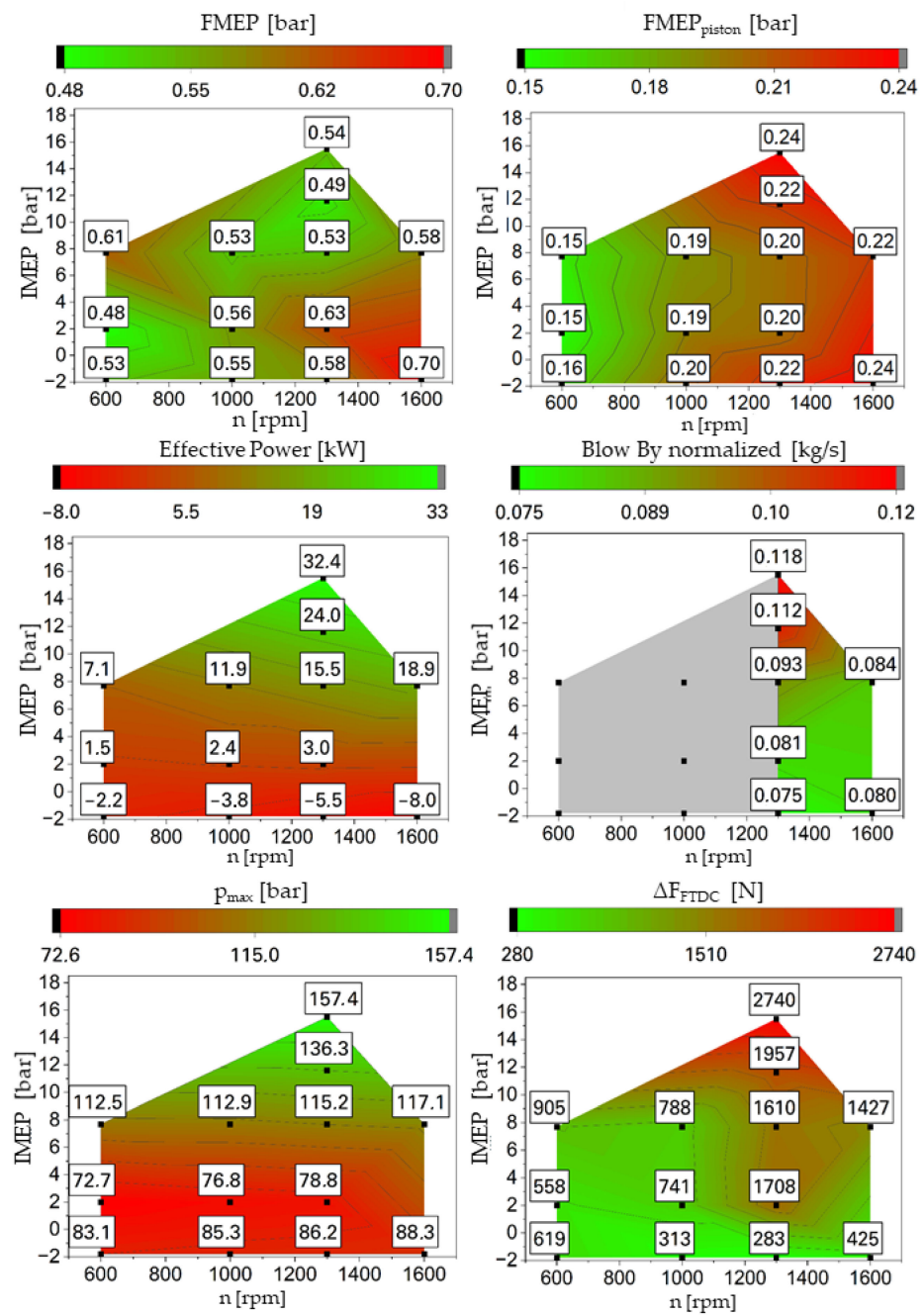


Figure 10. Measurement results for motored and fired operation conditions—free-form honed liner.

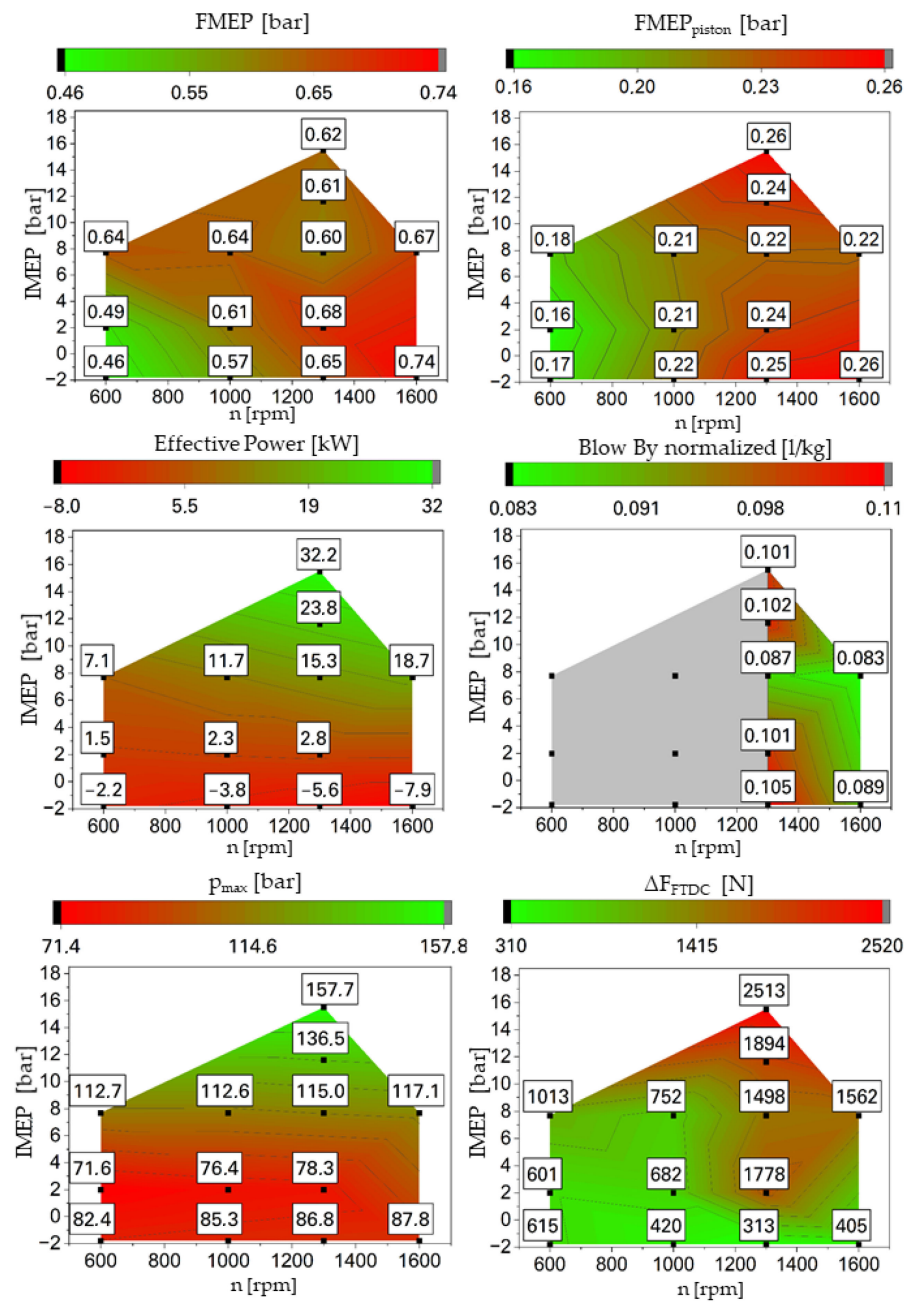


Figure 11. Measurement results for motored and fired operation conditions—reference liner.

4. Discussion

The following analysis will delve into the previously presented results, specifically examining the impact of the shape of the cylinder liner and investigating associated dependencies.

4.1. Influence Analysis through Investigations without Compression

Figure 12 exemplifies the friction force profile for an upward stroke (-180°CA – 0°CA) at 300 rpm without compression combined with a draft of the sectioned cylinder liner to depict the bore diameter in the warm operation state (only thermal deformation due to operation without compression).

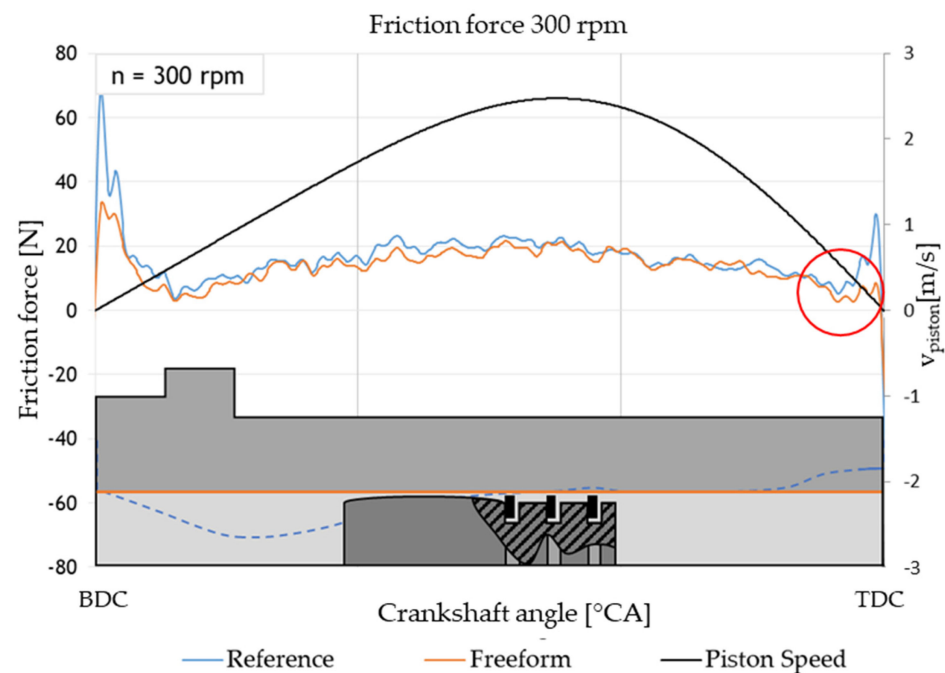


Figure 12. Friction force profile without compression at 300 rpm upward stroke.

The color codes for the sectioned cylinder liner correspond to the investigated variations in the cylinder liners and the friction force profiles. This representation aims to elucidate the influence of the varying bore diameters on the resulting friction force. In the hydrodynamic-predominated area, the free-formed honed liner shows slight advantages along the whole stroke. This is caused by the better alignment of the liner and the piston shaft over the height of the liner. Due to a larger lubrication gap, the shear stress is reduced. Towards the reversal points, the friction decreases for both liners due to slower piston speed. The minimum friction force can be associated with the Stribeck point, where the sum of hydrodynamic friction and boundary friction is minimal. For the reference liner, the Stribeck point towards the TDC is associated with a crankshaft angle of $\varphi \approx -10^\circ \text{CA}$. For the free-form honed liner, a Stribeck point with a lower relative velocity is evident (marked detail), resulting in an enlarged hydrodynamic section and a smaller wear-related boundary friction part. At the reversal points, the better circular shape of the free-form honed liner reduces the contact pressure of ring pretension and leads to less boundary friction. At this operation point, the circular advantage is more pronounced than the deformation over the height; otherwise, the contrary clearances in the BDC and the TDC would create contrary friction results. For this operation point, the thermal deformation of the liner is only influenced by the supply medium temperature. In the design of the free-form liner, however, combustion temperature and pressure of the operation point at 15.5 bar IMEP and 1300 rpm have been considered, leading to the assumption that the deformation of both liners over the height is rather similar for the shown operation point. The circular deformation, however, is compensated and shows the measured friction advantages. Comparing the BDC with the TDC, the friction force amplitude of both cylinder liner variants is greater when the piston is at rest at the BDC. This difference can be attributed to the asymmetric convexity of the compression rings and the piston, causing the behavior of the existing lubricant in the lubrication gap to vary with changes in relative velocity. The lower oil volume during the upward stroke must be considered, since only the non-scraped oil from the previous downward movement is available for lubrication. Furthermore, it is possible that the deformation in each region is different. This is indicated by the different advantages of the free-form liner due to its circular deformation compensation.

4.2. Influence Analysis through Investigations with Compression

To investigate friction forces under engine-operating conditions, the cylinder liners are compared for varying load points across speed and indicated mean pressure (IMEP) in the following exposition.

For exemplary representation of the friction force profiles, Figure 13 depicts the friction forces at the lowest speed, $n = 600$ rpm, without combustion. This minimizes the impact of oscillations on the overall trend in the measured data. This representation allows for a cycle-dependent analysis of friction forces. The friction force profiles over the 200 averaged working cycles show minimal macroscopic differences between the examined cylinder liners for the parts with higher velocity between the turning points. The effects elucidated in Section 4.1 for hydrodynamic friction between the reversal points are not continuously evident along the stroke. In the region near the TDC, significant increases in friction force are observed due to the compression cycle. The free-form liner shows clearly reduced friction from about -30°CA on, as it approaches the TDC. The improved roundness of the free form ensures an enlargement of the lubricating film-building surfaces of the piston rings, expanding the hydrodynamic region of friction. Despite the acting combustion chamber pressure, the collective load can be influenced in such a way that hydrodynamic friction persists at low relative velocities. Additionally, the force jump at the TDC for the free-form honed liner is smaller than that of the reference. This may result from the diminishing clearance and the consequent expansion of the hydrodynamic friction area at lower relative speeds, leading to a reduction in solid friction. This could additionally be supported by minimizing piston tilting, by a better guidance, leading to a substantial increase in the effective contact area and a decrease in contact pressure.

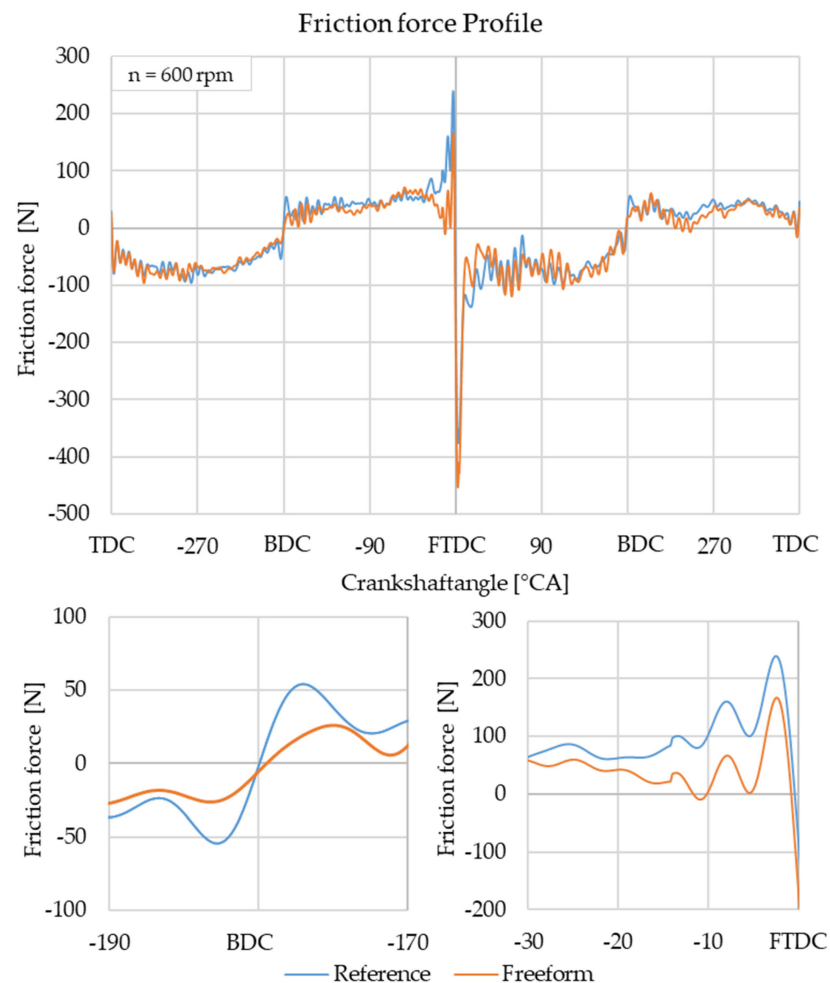


Figure 13. Friction force profile at 600 rpm (compressed case without combustion).

4.2.1. Analysis of Piston Group Friction

To analyze the friction reductions across the entire operating map, the percentage changes in piston group friction are depicted in Figure 14. The reference liner serves as the baseline for comparison. Figure 14 shows significant advantages for the free-form liner, particularly at low speeds and high indicated mean effective pressures. The most substantial reduction of 17.3% for the free-form honed cylinder liner occurs at a speed of $n = 600$ rpm and an indicated mean effective pressure of $IMEP = 7.7$ bar. The comparison shows, further, that the free-form variant induces reductions in piston group friction over the entire operating map. Here, the influence of the basic design idea is clearly visible. According to that design, the operated liner being heated from the combustion process has a form which is obviously nearer to a cylindrical shape, thus reducing the averaged friction. The presented results demonstrate that the designed free-form honed cylinder liner achieves significant reductions in the friction for the piston group of up to 17.3%, with an average reduction of 9.3% across the investigated operating map. This corresponds to an averaged power advantage of 0.103 kW.

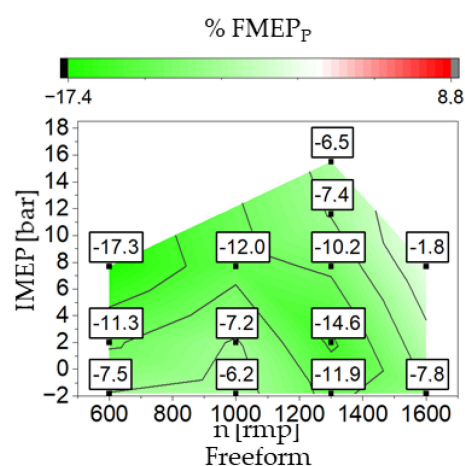


Figure 14. Percentage change in piston group friction for the free-form honed liner in comparison to the reference liner.

In order to analyze the difference in the friction forces in more detail, the direct visual comparison of the measured friction force is less easy than for the cases without combustion, as the force signal is biased by increasing oscillations. They have their source, on the one hand, from excitations of the Floating-Liner system, as the liner is partly movable in its upper part and forms its own dynamical system. On the other hand, the piston rings have their own dynamics, inducing some oscillations on the observed pressure signal. For the average friction, as has been evaluated before, these oscillations are suppressed due to the averaging over time. With some care, some observations can be made for the detailed friction process as a function of crankshaft angle. Figure 15 depicts a load of $IMEP = 7.7$ bar at a speed of $n = 600$ rpm for both the reference and the free-form honed cylinder liner as a function of the crankshaft angle. Due to the high piston speed in the mid-stroke range, and the existing hydrodynamic friction, a significant impact is observed. Additional disturbances from the combustion pressure occur during the combustion cycle, aligning in frequency, but complicating graphical interpretation. For a more detailed analysis, these areas are depicted separately for both the compression and combustion stroke. In this examination, a noticeable reduction in frictional force is evident in the higher combustion chamber pressures, which, due to the substantial volume change per crankshaft angle, exerts a significant influence on the $FMEP_p$. Additionally, due to the adapted shape of the free-form honing, a further reduction in friction is distinctly observed in the high combustion chamber pressure range. This relation results in reductions in frictional force of 13.1% for the compression stroke and 21.8% for the combustion stroke. The additional

reduction for the first and the fourth stroke in the hydrodynamic friction range results in an overall reduction of the $FMEP_p = 17.3\%$ for the depicted load point $IMEP = 7.7$ bar.

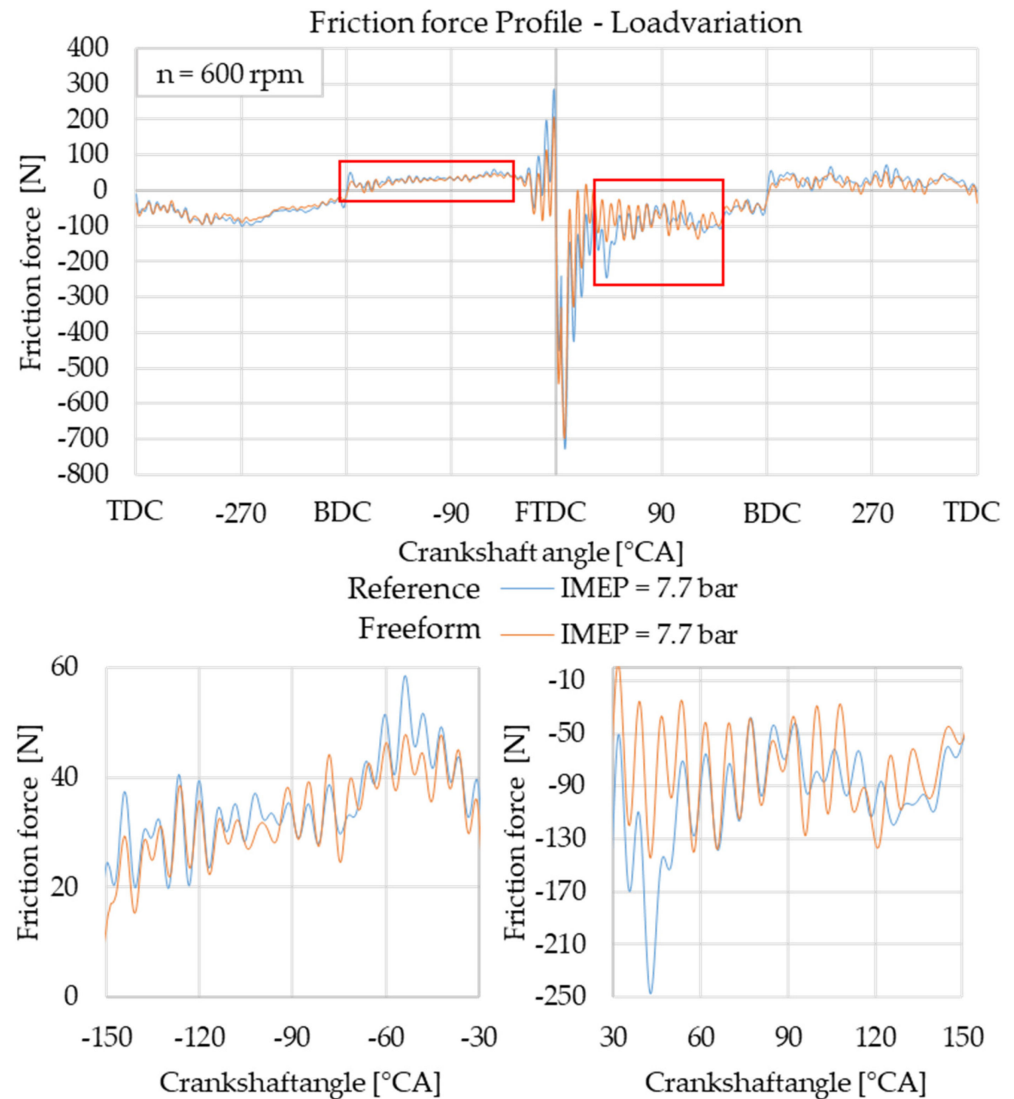


Figure 15. Friction force profile 600 rpm IMEP = 7.7 bar.

4.2.2. Analysis of the Peak Friction Force at the Fired Top Dead Center

To examine the peak friction forces at the fired top dead center (FTDC), the percentage changes are plotted in Figure 16. Additionally, the value of the friction force peaks serves as an indicator for wear characteristics. For the free-form honing, it becomes evident that reductions in the friction force jump can be achieved in the lower and upper speed range of the operating map. However, increases in the peak friction force are observed in the middle and upper range of the indicated mean pressure. This behavior suggests that the designed shape of the cylinder liner or the resulting shape from the manufacturing process is not optimally adapted to the thermal influences in this load range.

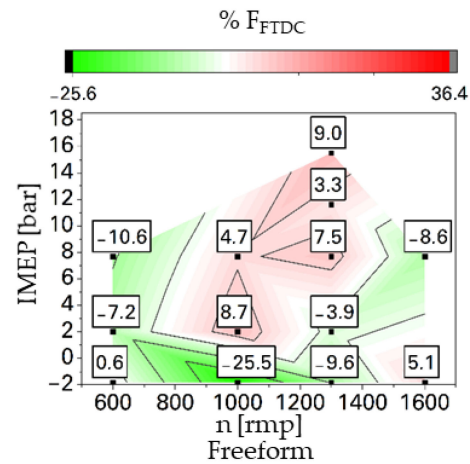


Figure 16. Percentage change in force at the FTDC for the free-form honed liner in comparison to the reference liner.

4.2.3. Analysis of Blow-By

Figure 17 presents the measured blow-by values for evaluating the sealing behavior of the piston group, again as the relative change in the free-formed liner in comparison to the reference liner. Due to the utilized measurement system, as indicated before and described in [11], only speeds $n > 1200$ rpm can be considered. Generally, the blow-by losses increase with higher indicated mean effective pressure, as the compression and combustion pressure increases. For the investigated free-form honed liner the increase in blow-by at high IMEP is even stronger than for the reference form, as can be seen in the relative change in the blow-by in Figure 17. For the highest operating point, the blow-by increases up to 16.9% of the reference. For lower IMEP, the free-form honed liner shows much smaller blow-by with measured reductions up to -28.8% . The measurements of the blow-by show an operating-point-dependent behavior, indicating a suboptimal design of the free-formed liner.

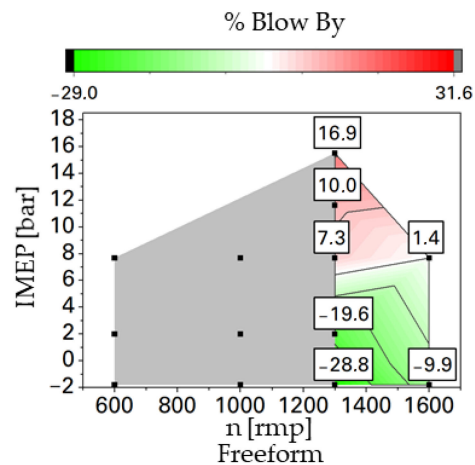


Figure 17. Percentage change in blow-by for the free-form honed liner in comparison to the reference liner.

5. Conclusions

The thermal and mechanical load on the cylinder liner of a piston engine leads to a deformation of the liner in the hot state. This deformation is composed of a deformation along the height of the liner and a radial deformation. A serial liner with its fully cylindrical inner shape in the cold state deforms to an unfavorable form in the hot state concerning the liner piston alignment. Better would be a free-formed cylinder liner, which is produced in the cold state in such a way that it reaches a nearly cylindrical shape in the hot operation

state. In this study, such a liner was produced with new and flexible honing tools, based on an earlier numerically based simulation of the deformation. This liner was investigated in detail on the heavy-duty Floating-Liner single-cylinder research engine at Leibniz University Hannover. For comparison, a reference liner was used with conventional cylindrical shape in the cold state. In conclusion, from the preceding explanations, it can be inferred that a free-form honed cylinder liner can reduce the losses due to piston group friction significantly over the whole investigated engine map. Here, up to 17.3% reductions have been observed for the free-form honed liner in comparison to a reference liner. For some operational points, wear improvement has also been achieved. This can be attributed to reduced mixed-friction areas of the free-form honed liner. Additionally, it has been demonstrated that the shape of the cylinder liner can influence leakage losses in the form of blow-by gas measurement in positive and negative directions. Despite the design point at 1300 rpm and 15.5 bar IMEP, the desired effect is not pronounced here, and an optimal approach in this respect still has to be found. The potential reductions in mechanical and thermal losses are strongly dependent on the operating conditions, making the greatest efficiency improvement expected for stationary applications for a certain design point. An optimization for a broader range of operation points will be a challenge. Very promising here is the result of reduced friction of about 9.3%, being averaged over all operation points. This shows, in summary, that free-form honed liners can lead to significant fuel savings and increased thermodynamic efficiency. The reduction in friction and possible oil consumption result in overall lowered CO₂ and oil-related emissions. Furthermore, the reduced wear of the lowered friction supports less energy consumption in the manufacturing process [10].

Author Contributions: Conceptualization, F.S. and F.P.-T.; methodology, F.S.; investigation, F.S. and F.P.-T.; resources, F.D.; data curation, F.S. and F.P.-T.; writing—original draft preparation, F.S.; writing—review and editing, F.P.-T. and F.D.; visualization, F.S.; supervision, F.D.; project administration, F.S.; funding acquisition, F.P.-T. and F.D. All authors have read and agreed to the published version of the manuscript.

Funding: The study is mostly funded research work from the German Federal Ministry for Economic Affairs and Energy (BMWi) within the cooperation project “Antriebsstrang 2025”. Partial funding is given from the Leibniz University Hannover.

Data Availability Statement: Data is partly available on request. The data are not publicly available due to privacy.

Acknowledgments: The authors would like to thank Henning Pasligh and Ahmad Alshwawra for sharing their experiences and fruitful discussions. Special thanks to the colleagues of the Institute of Production Engineering and Machine Tools (IFW).

Conflicts of Interest: The authors declare no conflicts of interest.

References

1. Merker, G.P.; Schwarz, C.; Teichmann, R. (Eds.) *Combustion Engines Development*; Springer: Berlin/Heidelberg, Germany, 2011.
2. Gangopadhyay, A. A Review of Automotive Engine Friction Reduction Opportunities through Technologies Related to Tribology. *Trans. Indian Inst. Met.* **2017**, *70*, 527–535. [[CrossRef](#)]
3. Edtmayer, J.; Lösch, S.; Hick, H.; Walch, S. Comparative Study on the Friction Behaviour of Piston/Bore Interface Technologies. *Automot. Engine Technol.* **2019**, *4*, 101–109. [[CrossRef](#)]
4. Alshwawra, A.; Pohlmann-Tasche, F.; Stelljes, F.; Dinkelacker, F. *Cylinder Liner Deformation—An Investigation of Its Decomposition Orders under Varied Operational Load*; Technical Paper 2022-01-1040; SAE: Warrendale, PE, USA, 2022. [[CrossRef](#)]
5. Maisch, C.; Böhm, H.-P. *Konturhonen auf dem Prüfstand, Experten-Forum Powertrain 2020*; Springer: Hanau, Germany, 2020.
6. Koch, F.; Decker, P.; Gülpen, R.; Quadflieg, F.-J.; Loeprecht, M. *Cylinder Liner Deformation Analysis Measurement and Calculation*; Technical Paper 980567; SAE: Warrendale, PE, USA, 1998. [[CrossRef](#)]
7. Yamada, T.; Kobayashi, H.; Kusama, K.; Sagawa, J. *Development of Technique to Predict Oil Consumption with Consideration for Cylinder Deformation*; Technical Paper 2003-01-0982; SAE: Detroit, MI, USA, 2003.
8. Fujimoto, H.; Yoshihara, Y. *Measurement of Cylinder Bore Deformation Firing Actual Operating Engines*; Technical Paper 910042; SAE: Detroit, MI, USA, 1991.
9. Berg, M.; Schultheiß, H.; Musch, D.; Hilbert, T. Moderne Methoden zur Optimierung von Zylinderverzügen. *Mot. Z.* **2015**, *12*, 46–55. [[CrossRef](#)]

10. Barbieri, S.G.; Giacopini, M.; Mangeruga, V.; Bianco, L.; Mastrandrea, L.N. A Simplified Methodology for the Analysis of the Cylinder Liner Bore Distortion: Finite Element Analyses and Experimental Validations. In Proceedings of the 14th International Conference on Engines & Vehicles, Napoli, Italy, 15–19 September 2019; SAE International: Warrendale, PE, USA, 2019. [CrossRef]
11. Selmani, E.; Delprete, C.; Bisha, A. Cylinder Liner Deformation Orders and Efficiency of a Piston Ring-Pack. *E3S Web Conf.* **2019**, *95*, 04001. [CrossRef]
12. Flores, G.K. *Graded Freeform Machining of Cylinder Bores Using Form Honing*; Technical Papers 2015-01-1725; SAE: Warrendale, PE, USA, 2015. [CrossRef]
13. Hrdina, D.; Maurizi, M.; Lemm, B.; Kahraman, H.; Doares de Faria, G. *Variably Honed Cylinder Liners, Iron-Based Cast Pistons and Variably Coated Piston Rings as PCU System for Friction Loss and TCO Reduction*; Springer: Stuttgart, Germany, 2019.
14. Edtmayer, J.; Walch, S.; Lösch, S.; Jech, M.; Wopelka, T. *Implementierung Einer Kombinierten Verschleiß- und Reibanalyse an Einem Einzylinder-Forschungsmotor*; Springer: Wiesbaden, Germany, 2017.
15. MS Motorservice Deutschland GmbH, MS Motorservice. Available online: https://www.ms-motorservice.com/MediaAssets/1449287_ks_50003958-01_web.pdf (accessed on 28 February 2024).
16. Forbes, J.E.; Taylor, E.S. *A Method for Studying Piston Friction*; NACA Wartime Report No. W-37; NACA: Boston, MA, USA, 1943.
17. Denkena, B.; Poll, G.; Dinkelacker, F.; Handrup, M.; Katzsch, D.; Meyer, K.; Pillkahn, P.; Reuter, L.; Schmidt, C.; Stelljes, F. *Antriebsstrang 2025: Energieeffiziente Prozessketten zur Herstellung eines Reibungs-, Gewichts- und Lebensdaueroptimierten Antriebsstrangs*; Abschlussbericht (Final Report) zum BMWK-Verbundprojekt; Institutionelles Repositorium der Leibniz Universität Hannover: Hannover, Germany, 2023. [CrossRef]
18. Alshwawra, A. Development of Advanced Cylinder Liner Conformation Concepts of Internal Combustion Engines with Numerical Simulation Methods. Doctoral Dissertation, Leibniz Universität Hannover, Hannover, Germany, 2023. [CrossRef]
19. Alshwawra, A.; Pohlmann-Tasche, F.; Stelljes, F.; Dinkelacker, F. Effect of Freeform Honing on the Geometrical Performance of the Cylinder Liner—Numerical Study. *SAE Int. J. Engines* **2022**, *16*, 463–486. [CrossRef]
20. Schmidt, C. Prozessentwicklung zur Tribologischen Funktionalisierung von Nutzfahrzeug-Zylinderlaufbuchsen. Doctoral Dissertation, Leibniz Universität Hannover, Hannover, Germany, 2024. planned.
21. Denkena, B.; Schmidt, C.; Meyer, K. *Reduzierung der Treibhausgasemission durch Energieeffiziente Prozessketten für die Herstellung von Antriebsstrangkomponenten*, 5th ed.; Fachtagung Sensitive Fertigungstechnik: Magdeburg, Germany, 2019.
22. Denkena, B.; Dittrich, M.-A.; Bergmeier, M.; Handrup, M.; Meyer, K.; Onken, L.; Schmidt, C. Energy Efficient Process Chains for the Production of Powertrains. In Proceedings of the 17th Global Conference on Sustainable Manufacturing, Shanghai, China, 9–11 October 2019. [CrossRef]
23. Denkena, B.; Bergmann, B.; Handrup, M.; Schmidt, C. Controlled Turning Process for the Production of Friction-Reduced Cylinder Liners with a Defined Free-Form Geometry. *J. Mach. Eng.* **2021**, *21*, 47–59. [CrossRef]
24. Denkena, B.; Bergmann, B.; Handrup, M. Piezo-actuated hybrid tool for the micro structuring of cylinder liners in an energy-efficient process chain. In Proceedings of the 5th International Conference on System-Integrated Intelligence, Bremen, Germany, 11–13 November 2020.
25. Pasligh, H. Tribologisch maßgeschneiderte Zylinderlaufbuchse durch Oberflächenstrukturierung bei Nutzfahrzeugen. Doctoral Dissertation, Leibniz Universität Hannover, Hannover, Germany, 2021.
26. Ulmer, H. Einfluss Mikrostrukturierter Zylinderlaufbahnen auf die Tribologie der Kolbengruppe bei Nutzfahrzeug Dieselmotoren. Doctoral Dissertation, Leibniz Universität Hannover, Hannover, Germany, 2015.
27. Pohlmann-Tasche, F.; Stelljes, F.; Dinkelacker, F. *Reibungsoptimierung der Kolbengruppe bei Nutzfahrzeug-Verbrennungsmotoren*, 30th ed.; Dinkelacker, F., Pitsch, H., Scherer, V., Eds.; Deutscher Flammentag—Für Nachhaltige Verbrennung: Hannover-Garbsen, Germany, 2021; pp. 789–795.
28. Koeser, P.; Berbig, F.; Pohlmann-Tasche, F.; Pasligh, H.; Dinkelacker, F. *Predictive Piston Cylinder Unit Simulation—Part I: Novel Findings on Cyclic Inter-Ring Pressure Measurements and Piston Ring Dynamic Simulation Validation*; SAE Technical Paper 2021-01-0650; SAE: Warrendale, PE, USA, 2021. [CrossRef]
29. Furuhashi, S. *Measurement of Piston Frictional Force in Actual Operating Diesel Engine*; SAE 790855; Tokio: Tokyo, Japan, 1979.
30. Halsband, M. Entwicklung reibungsoptimierter Kolbengruppen unter Anwendung spezifischer Messverfahren. *VDI-Fortschrittsberichte* **1994**, *12*, 221.
31. Kessen, U. Tribologische Untersuchung an der Kolbengruppe eines Dieselmotors bei Hohen Mitteldrücken. Doctoral Dissertation, Leibniz Universität Hannover, Hanover, Germany, 1999.
32. Tischbein, H.W. Reibung an Kolbenringen. Doctoral Dissertation, Technische Hochschule Karlsruhe, Karlsruhe, Germany, 1939.
33. Heywood, J.B. *Internal Combustion Engine Fundamentals*; McGraw-Hill: New York, NY, USA, 1988.
34. Küntschner, V.; Hoffmann, W. *Kraftfahrzeugmotoren: Auslegung und Konstruktion*, 5th ed.; Vogel Business Media: Würzburg, Germany, 2014.

Disclaimer/Publisher’s Note: The statements, opinions and data contained in all publications are solely those of the individual author(s) and contributor(s) and not of MDPI and/or the editor(s). MDPI and/or the editor(s) disclaim responsibility for any injury to people or property resulting from any ideas, methods, instructions or products referred to in the content.